doi:10.26443/seismica.v4i1.1347

SEISMICA

The impact of COVID-19 lockdown measures on high-frequency seismic ambient noise in Greece: Utilizing strong-motion seismograph networks for human activity monitoring in urban environments

Dimitrios Giannopoulos * [1], **Christos P. Evangelidis** [2], **Efthimios Sokos** [1]

[1]Laboratory of Seismology, Department of Geology, University of Patras, Patras, Greece , [2]Institute of Geodynamics, National Observatory of Athens, Athens, Greece

Author contributions: *Formal Analysis*: D. Giannopoulos, C. Evangelidis. *Methodology*: D. Giannopoulos, C. Evangelidis. *Software*: D. Giannopoulos, C. Evangelidis. *Visualization*: D. Giannopoulos. *Writing - Original draft*: D. Giannopoulos. *Writing - Review & Editing*: D. Giannopoulos, C. Evangelidis, E. Sokos. *Supervision*: C. Evangelidis, E. Sokos.

Production Editor:
Gareth Funning
Handling Editor:
Lise Retailleau
Copy & Layout Editor:
Anant Hariharan

Received:
January 4, 2025
Accepted:
May 15, 2025
Published:
June 12, 2025

Abstract Vibrations generated by anthropogenic activity propagate into the Earth's subsurface as high-frequency seismic waves. The COVID-19 pandemic, which prompted widespread adoption of prevention policies in 2020, including social distancing measures, stay-at-home orders, travel restrictions and lockdowns, provided a unique opportunity to investigate on a country-scale the impact of the pandemic restriction measures on seismic data. Greece, which implemented two strict nationwide lockdowns in March and November 2020, serves as a case study for examining the effects of the two national lockdown measures on high-frequency ambient seismic noise. We analyze seismic waveform data obtained exclusively from strong-motion seismic sensors deployed in urban areas across Greece. Our findings reveal a significant 43% reduction in seismic noise levels during the first lockdown and a slightly less, yet still substantial, reduction of 36% during the second lockdown. The most substantial daily reduction in seismic noise levels, exceeding 80%, occurred on Easter Sunday of 2020, during the first lockdown. The decrease in human activity during the 2020 lockdowns resulted in the most extensive and prolonged reduction in anthropogenic seismic noise ever recorded on a national scale in Greece. Our results highlight the effectiveness of strong-motion accelerograph stations in monitoring the effects of lockdown measures on seismic data. Notably, co-located acceleration and broadband sensors exhibited similar variations in high-frequency seismic noise. Furthermore, a strong correlation between high-frequency seismic noise and various categories of human mobility suggests the potential utility of accelerometers in long-term seismic monitoring of human activity.

Second Language Abstract: Σύνοψη (Greek)

Οι δονήσεις που προκαλούνται από ανθρωπογενείς δραστηριότητες διαδίδονται στο υπέδαφος ως σεισμικά κύματα υψηλής συχνότητας. Το 2020, η πανδημία COVID-19, η οποία οδήγησε στην ευρεία εφαρμογή μέτρων πρόληψης, όπως η κοινωνική αποστασιοποίηση και οι περιορισμοί κυκλοφορίας, προσέφερε μια μοναδική ευκαιρία για τη μελέτη της επίδρασης αυτών των περιοριστικών μέτρων στα σεισμικά δεδομένα σε εθνική κλίμακα. Η Ελλάδα, η οποία εφάρμοσε δύο καθολικές απαγορεύσεις κυκλοφορίας (lockdowns) τον Μάρτιο και τον Νοέμβριο του 2020, αποτελεί μία μελέτη περίπτωσης για την εξέταση της επίδρασης των περιοριστικών αυτών μέτρων στον υψηλής συχνότητας σεισμικό θόρυβο. Αναλύσαμε σεισμικά δεδομένα που καταγράφηκαν αποκλειστικά από επιταχυνσιογράφους εγκατεστημένους σε αστικές περιοχές της Ελλάδας. Τα αποτελέσματα δείχνουν ότι σημειώθηκε σημαντική μείωση 43% στα επίπεδα σεισμικού θορύβου κατά τη διάρκεια της πρώτης απαγόρευσης κυκλοφορίας και μια ελαφρώς μικρότερη, αλλά εξίσου σημαντική, μείωση 36% κατά τη διάρκεια της δεύτερης απαγόρευσης κυκλοφορίας. Η μεγαλύτερη ημερήσια μείωση στα επίπεδα σεισμικού θορύβου, η οποία ξεπέρασε το 80%, καταγράφηκε την Κυριακή του Πάσχα του 2020, κατά τη διάρκεια της πρώτης απαγόρευσης κυκλοφορίας. Η μείωση της ανθρώπινης δραστηριότητας κατά τη διάρκεια των απαγορεύσεων κυκλοφορίας του 2020 οδήγησε στη μεγαλύτερη και πιο παρατεταμένη μείωση ανθρωπογενούς σεισμικού θορύβου που έχει καταγραφεί ποτέ σε εθνική κλίμακα στην Ελλάδα. Τα αποτελέσματα αναδεικνύουν, μεταξύ άλλων, την αποτελεσματικότητα των επιταχυνσιογράφων στην παρακολούθηση της επίδρασης των περιοριστικών μέτρων στα σεισμικά δεδομένα. Είναι αξιοσημείωτο ότι οι συνεγκατεστημένοι επιταχυνσιογράφοι και σεισμογράφοι ευρέος φάσματος παρουσίασαν παρόμοιες μεταβολές στον σεισμικό θόρυβο υψηλών συχνοτήτων, κάτι που ενισχύει την αξιοπιστία των μετρήσεων. Επιπλέον, η ισχυρή συσχέτιση που παρατηρήθηκε μεταξύ της μεταβολής των επιπέδων του σεισμικού θορύβου και των δεδομένων ανθρώπινης κινητικότητας υποδηλώνει τη δυνητική χρησιμότητα των επιταχυνσιογράφων στη μακροπρόθεσμη σεισμική παρακολούθηση της ανθρωπογενούς δραστηριότητας.

1 Introduction

The emergence of human cases of an upper respiratory tract infection caused by a novel coronavirus (SARS-CoV-2), officially abbreviated as COVID-19 (coronavirus disease 2019) by the World Health Organization (WHO), was initially reported by national authorities in the city of Wuhan, Hubei Province in China, in December 2019 (Li et al., 2020). Subsequently, the virus rapidly spread globally in the following months. By the beginning of March 2020, the WHO had formally declared the COVID-19 outbreak a global pandemic. The COVID-19 pandemic has sparked major health, social, economic, and humanitarian crises, and has rapidly evolved into one of humanity's most profound challenges in the 21st century. As of May 2023, the WHO has downgraded the COVID-19 pandemic, reporting that the disease no longer qualifies as a public health emergency of international concern.

Similar to many other affected countries, Greece aimed to mitigate the spread of COVID-19 by gradually implementing public health scenarios, including restrictive measures on citizens' mobility. These measures commenced on March 11, 2020, with the closure of educational institutions. Subsequently, restaurants and shopping centers were closed on March 13, 2020, leading to the declaration of a nationwide lockdown (hereafter LD1) on March 23, 2020. The containment measures for LD1 were lifted after 43 days, on May 4, 2020. In response to the resurgence of a severe second wave of COVID-19 cases towards the end of 2020, Greek authorities implemented a second nationwide lockdown (hereafter LD2) on November 7, 2020. Following the implementation formula of LD1, all non-essential activities were once again suspended across the entire country. A detailed overview of the major phases of COVID-19 emergency measures in Greece is presented in Table 1.

In seismology, two types of signals are considered to constitute random wave fields. The first comprises seismic coda waves, which are mainly the multiple scattered parts of the seismic waveforms (Paul et al., 2005). The second category involves seismic noise, which refers to signals recorded in the absence of identifiable active sources, superimposing on all recorded seismic data (Curtis et al., 2006). The latter, independent of earthquake activity, is recorded by seismometers globally and continuously in time (Stutzmann et al., 2000; Gualtieri et al., 2013). This continuous background seismic noise primarily comes from two different origins, natural or human-made, and its classification is primarily based on its frequency content. According to a principal categorization, frequencies smaller than 1 Hz are associated with natural seismic noise sources (e.g., atmospheric and ocean activity), and at intermediate frequencies between 1 and 5 Hz, the sources include both natural (e.g., local meteorological conditions, storms) or human-made factors (e.g., urban activities, industrial processes). Frequencies higher than approximately 5 Hz are predominantly associated with cultural or anthropogenic sources (Bonnefoy-Claudet et al., 2006, and references therein). There are, however, cases of seismic noise sources that fall outside this primary categorization. For example, low-frequency seismic background noise (0.01–0.05 Hz) observed at broadband seismic stations has been shown to strongly correlate with railway schedules (Sheen et al., 2009).

An aftereffect of the COVID-19 pandemic lockdowns and the subsequent temporary restrictions on non-essential activities was notable reductions in anthropogenic seismic noise, which is continuously monitored by the seismological networks. The seismic signature of this phenomenon was initially documented on a global scale by Lecocq et al. (2020a). Their analysis of high-frequency seismic ambient noise (HiFSAN, as abbreviated in Lecocq et al. (2020a)) revealed a substantial decrease in its global median, approximately 50%, from March to May 2020, coinciding with the implementation of full lockdowns in many countries worldwide. Similarly, variations of HiFSAN energy in relation to the implementation of lockdown measures were also documented by various regional and local-scale studies in Italy (Poli et al., 2020; Cannata et al., 2021), Spain (Diaz et al., 2021), Greece (Giannopoulos et al., 2021, 2022), Central America (De Plaen et al., 2021; Arroyo-Solórzano et al., 2021; Pérez-Campos et al., 2021), South America (Diaz et al., 2020; Ojeda and Ruiz, 2021), Japan (Yabe et al., 2020), China (Xiao et al., 2020), Russia (Boginskaya and Kostylev, 2022), and India (Somala, 2020).

In this study, we aim to assess the impact of COVID-19 pandemic lockdown measures on HiFSAN in Greece. The analysis is conducted on a national scale, utilizing continuous recording data exclusively acquired by strong-motion seismic sensors. We focus on examining how the two nationwide lockdowns implemented by the Greek government in 2020 affected seismic noise levels. Urban areas, comprising towns and cities, benefit from the presence of strong-motion seismic instruments, primarily utilized for monitoring strong ground motion parameters, conducting on-site structural health monitoring of public buildings and classical earthquake monitoring. Consequently, these environments are deemed ideal for monitoring anthropogenic seismic noise. Beyond our core objective, this study seeks to underscore the potential of strong-motion seismograph networks for long-term seismic monitoring of human activities.

2 Material and Methods

2.1 Data

The initial seismic noise dataset was compiled using vertical component waveform data obtained from 72 strong-motion seismic stations (Figure 1). These stations are part of the following networks: *i)* the Hellenic Seismic Network (HL) operated by the Institute of Geodynamics of the National Observatory of Athens, *ii)* the ITSAK strong-motion network (HI) operated by the Institute of Engineering Seismology & Earthquake Engineering and *iii)* the EUROSEISTEST Strong Motion Network (EG) operated by the Aristotle University of Thessaloniki. The stations were selected based on the public availability of their data at the time of analysis, as well

*Corresponding author: dgiannopoulos@upatras.gr

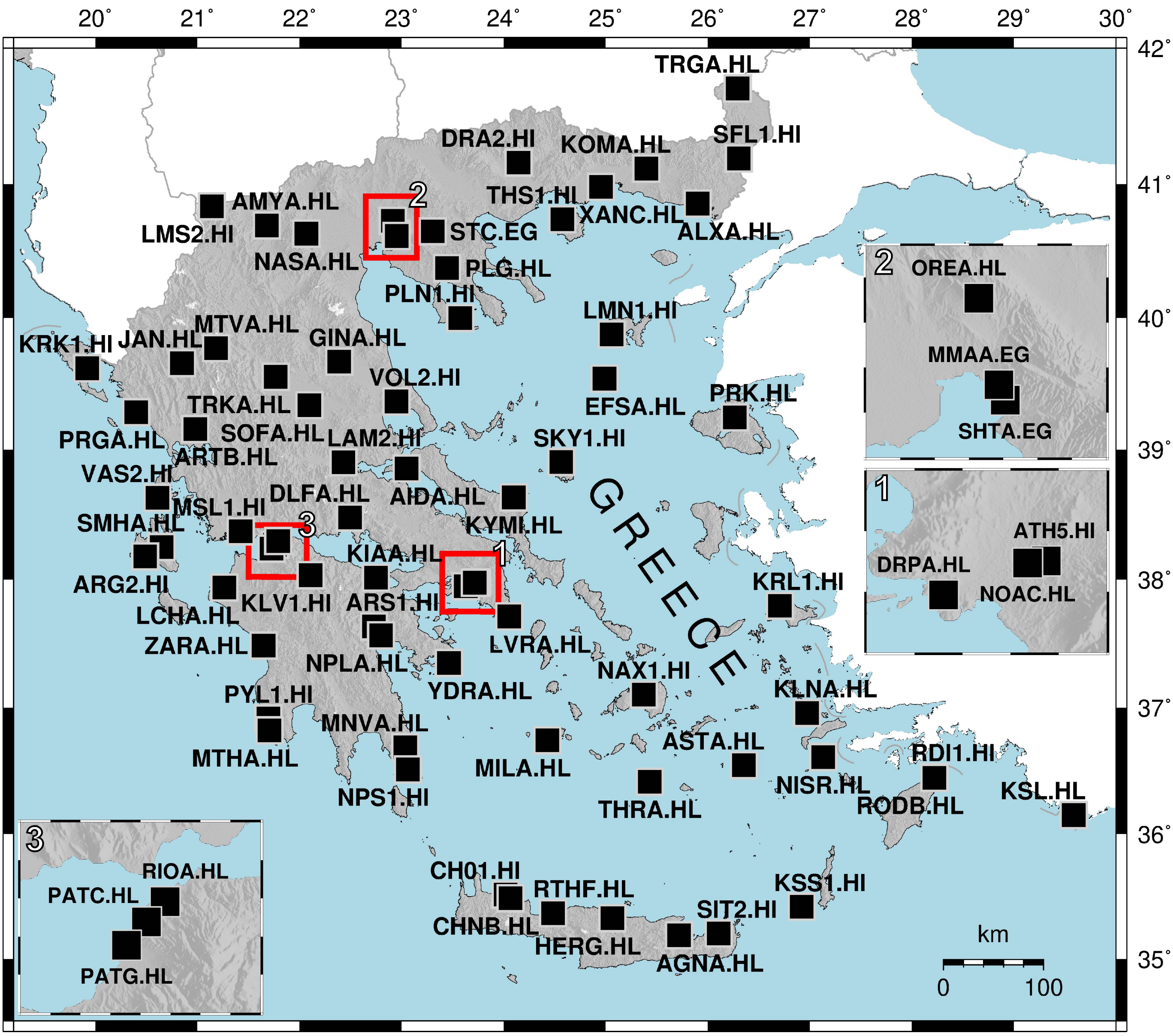

Figure 1 Map of Greece illustrating the locations of the strong-motion seismic stations (black squares) used in this study. Each station is labelled with a naming convention defined as "STA.NET", where STA is the station code and NET is the network code.

as their operation in continuous recording mode. Data from strong-motion stations that operate in triggering mode were excluded from the analysis, as such data are unsuitable for a long-term seismological monitoring effort. The selected stations are equipped with Güralp 5TDE strong-motion accelerometers, acquiring data at sampling rates between 100 and 250 samples per second (sps). All stations are located within towns, cities, or infrastructures, specifically installed in public buildings. A list of the specific type of building where the stations are installed is provided in the supplementary material. The installation of seismological stations within or near urban environments is typically considered a disadvantage for classical seismological analysis. Earthquake signals are often masked by large background noise produced by human activities. However, for the purpose of monitoring anthropogenic activity within the scope of the current study, this condition proves to be a significant advantage. The time interval of the analysis spans from November 1, 2019, to December 31, 2020 (14 months), covering the periods of the two national lockdowns (LD1 and LD2, see Table 1).

2.2 Seismic noise analysis

To investigate the temporal variations of the HiFSAN amplitude, we adopted the noise computation approach proposed by Lecocq et al. (2020a), analysing day-long seismic recordings from each station. The data were segmented into 30-minute windows with a 50% overlap and we estimated the power spectral density (PSD) of each windowed time series using Welch's method (Welch, 1967). PSD calculations were performed using the ObsPy (Krischer et al., 2015) implementation of the analogous routine proposed by McNamara and Buland (2004) and McNamara et al. (2009). Following Lecocq et al. (2020a), we applied less smoothing for the PSD calculations to enhance frequency resolution and obtain

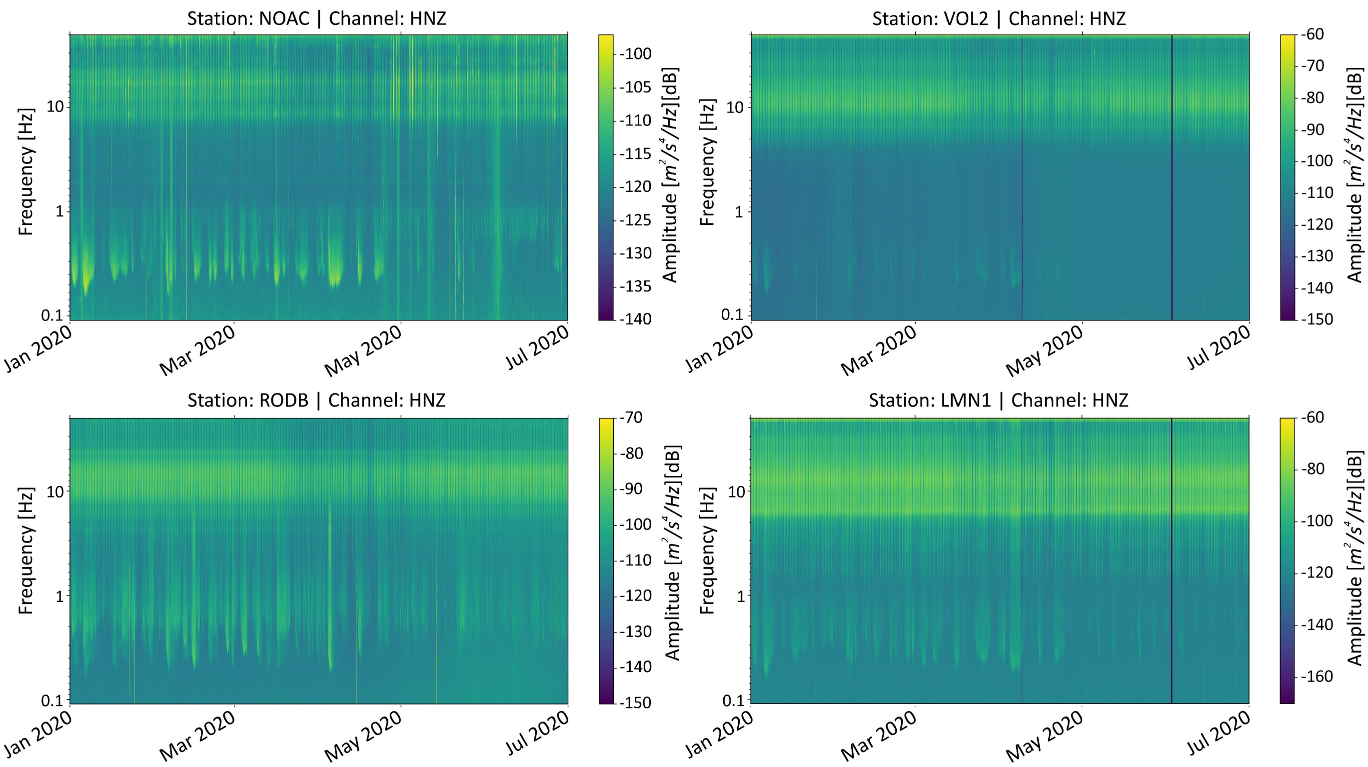

Figure 2 Spectrograms of the vertical component (HNZ) of seismic signals recorded by strong motion stations NOAC, VOL2, RODB and LMN1 from January 1 to June 30, 2020.

more dynamic power spectra. The acceleration PSDs were then converted to displacement spectral power. Utilizing Parseval's identity, the power spectral amplitudes were converted into root-mean-squares (rms) time series of the time-domain displacement across various frequency bands of interest. For visualization and comparison purposes, each calculated seismic noise displacement time series is accompanied by the corresponding moving median (window size: 24 hrs). The results of this analysis are presented and discussed in the following sections. For a more detailed description of the noise computation approach, refer to the Supplementary Materials of Lecocq et al. (2020a).

3 Results and Discussion

3.1 Selection of frequency band

To ascertain the influence of the COVID-19 lockdown measures on seismic noise, it is crucial to determine a frequency range where the impact of human activity on seismic data is most noticeable. A preliminary yet comprehensive assessment of the frequency content of seismic waveforms can be achieved through visual examinations of spectrograms. Figure 2 illustrates examples of spectrograms derived from four representative stations spanning the period from January 1 to July 1, 2020. Among these stations, NOAC and VOL2 are located in mainland Greece (Figure 1), within the city centers of Athens and Volos, respectively. The other two stations, RODB and LMN1, are located in the principal towns of the islands of Rhodes and Lemnos, respectively. While strong-motion sensors are typically designed to resolve large-amplitude, high-frequency seismic energy characteristic of large local earthquakes, the spectrograms reveal distinct spectral features in a frequency range commonly referred to as the secondary ocean-generated microseismic frequency band (< 1 Hz). Additionally, a pronounced feature in the spectrograms, likely originating from human-related activity, becomes apparent at frequencies above approximately 1 Hz, with notable dominance at frequencies above approximately 8 Hz (Figure 2).

Throughout the analysis, various frequency bandpass filters (4-14 Hz, 4-20 Hz, 5-25 Hz, 10-30 Hz, 20-45 Hz) were evaluated at most stations. For stations acquiring data at a sampling rate of 250 sps, the 50-90 Hz frequency band was also tested. Considering the proximity of the island stations to the sea and the fact that every station on mainland Greece is within a maximum distance of 150 km from the sea, the high-pass corner frequencies of the filters were set higher than 4 Hz. This was done to reduce potential contamination from the microseism energy of local seas (Evangelidis and Melis, 2012).

Figure 3 provides an overview of the long-term temporal evolution of HiFSAN influenced by different frequency bands, illustrated by examples from three representative stations (NOAC, PATG, OREA) spanning the time period from November 2019 to December 2020. The NOAC station, located in the city center of Athens within the facilities of the Institute of Geodynamics of the National Observatory of Athens, shows distinct drops in HiFSAN during LD1 and LD2 in all frequency bands except for the 50-90 Hz band (Figure 3a). Although post-lockdown HiFSAN levels at NOAC station appear to be lower than the pre-lockdown ones in the 50-90 Hz band, the interpretation of the overall varia-

Milestone Dates	Description
March 11, 2020	MD1: Closure of all educational institutions, including schools and universities.
March 13, 2020	MD2: Closure of all shopping centers, cafes, restaurants, bars, museums, and archaeological sites, with the exception of supermarkets and pharmacies.
March 23, 2020	**LD1 - 1st National Lockdown**: Suspension of all non-essential activities nationwide. Movement was strictly allowed only for six prescribed reasons: **i)** visits to doctors/pharmacies, **ii)** shopping for basic necessities from supermarkets, **iii)** visits to banks if online transactions were not possible, **iv)** providing assistance to people in need, **v)** travel to ceremonies (e.g., funerals, weddings) and **vi)** for outdoor physical exercise or walking pets, limited to maximum two people groups.
May 4, 2020	MD3: Beginning of gradual lifting of the restrictive measures on citizens' movement and business activity. People were permitted to move freely within their regional unit where they lived or worked. The overall plan for lifting restrictions included several milestone dates and extended until the beginning of June 2020, when hotels/touristic facilities (June 1, 2020) and indoor restaurants/cafes (June 6, 2020) resumed operations.
November 7, 2020	**LD2 - 2nd National Lockdown**: Suspension of all non-essential activities across the entire country, following the implementation formula of the 1st lockdown. The lifting of the emergency measures in this case was a prolonged process that continued until June 1, 2021, with the full-scale reopening of the tourism sector.

Table 1 Description of the key phases of the national emergency measures for COVID-19 in Greece, which significantly impacted citizens' mobility (Ministry of Health, 2022).

tion of HiFSAN in this band is challenging. Additionally, several narrow spikes are observed at frequencies below 10 Hz, possibly attributable to local weather conditions or data transmission problems, issues that are not relevant to the present study. At the PATG station, situated in the branch facilities of the Public Power Corporation in the city center of Patras, clear reductions in seismic noise are evident after both lockdowns (Figure 3b). The temporal variation of HiFSAN shows notable consistency across all examined frequency bands, with particularly prominent lockdown effects observed in the 50-90 Hz band, in contrast with the NOAC station. Similarly, the OREA station, situated in the Town Hall building of Oreokastro town near Thessaloniki city, exhibits an overall reduction in HiFSAN during the lockdowns across all frequency bands (Figure 3c). Noise reductions at the OREA station are relatively more pronounced in certain frequency bands (e.g., 10-30 Hz) compared to others (e.g., 20-45 Hz).

The lockdown effects on seismic noise are effectively captured across all studied frequency ranges, as shown in Figure 3. However, individual station examples may reveal variations among frequency ranges, likely influenced by local factors such as the frequency content of anthropogenic noise specific to each station, or other site-specific characteristics beyond the scope of this study. To better facilitate the presentation and visualization of the results, we focused our analysis on the 10-30 Hz frequency range. Additional results regarding the variations in seismic noise across other frequency ranges are provided in the supplementary material. It is worth noting that previous studies on this topic have similarly explored different bandpass filters to identify the optimal frequency band for presenting the influence of COVID-19 containment measures on seismic data. For instance, Lecocq et al. (2020a), Arroyo-Solórzano et al. (2021), De Plaen et al. (2021) and Ojeda and Ruiz (2021) have found a more pronounced impact in the 4-14 Hz frequency range. Cannata et al. (2021) concentrated on the 10-40 Hz frequency range, Pérez-Campos et al. (2021) on the 1-5 Hz range, Diaz et al. (2021) on the 2-20 Hz range, while Grecu et al. (2021) focused on the 15-40 Hz frequency range. The variations in the selected frequency bands among the aforementioned studies can be attributed to several factors, including differences in microseism influence on seismic data, variations in the locations of the seismic stations (e.g., rural or city-based), and differences in the types of seismological instruments employed. However, it is important to note that all studies aimed to mitigate potential secondary microseism contamination by focusing their analyses on frequencies greater than 1 Hz.

3.2 Seismic noise levels during COVID-19 lockdowns

3.2.1 General HiFSAN trends

Before discussing the generic trends in HiFSAN variation during the lockdowns, we can review some of the most characteristic trends observed in the long-term temporal evolution of HiFSAN during the analysis. Figure 4 provides examples of ground displacement variations for the entire analysis period from four representative stations in the selected 10-30 Hz frequency range.

Station AMYA demonstrates a typical HiFSAN variation pattern, clearly capturing both lockdown effects (Figure 4a). Significant noise reductions are observed at station AMYA after the implementation of both LD1 and LD2. Therefore, station AMYA serves as a case example of a station where both lockdown effects are clearly visible. Notably, the vast majority of stations in the current analysis exhibit similar patterns, demonstrating reductions in noise during both lockdowns. However, at very few stations, a different HiFSAN variation pattern is observed, such that only one of the two lockdown effects is clearly evident. Examples of this include stations ARTB (Figure 4b) and LMS2 (Figure 4c), where noise reduction was more prominent during only LD1 or LD2, respectively. This observation likely reflects varying levels of anthropogenic activity within the vicinity of the seismic stations during each lockdown period. This could include mobility changes both

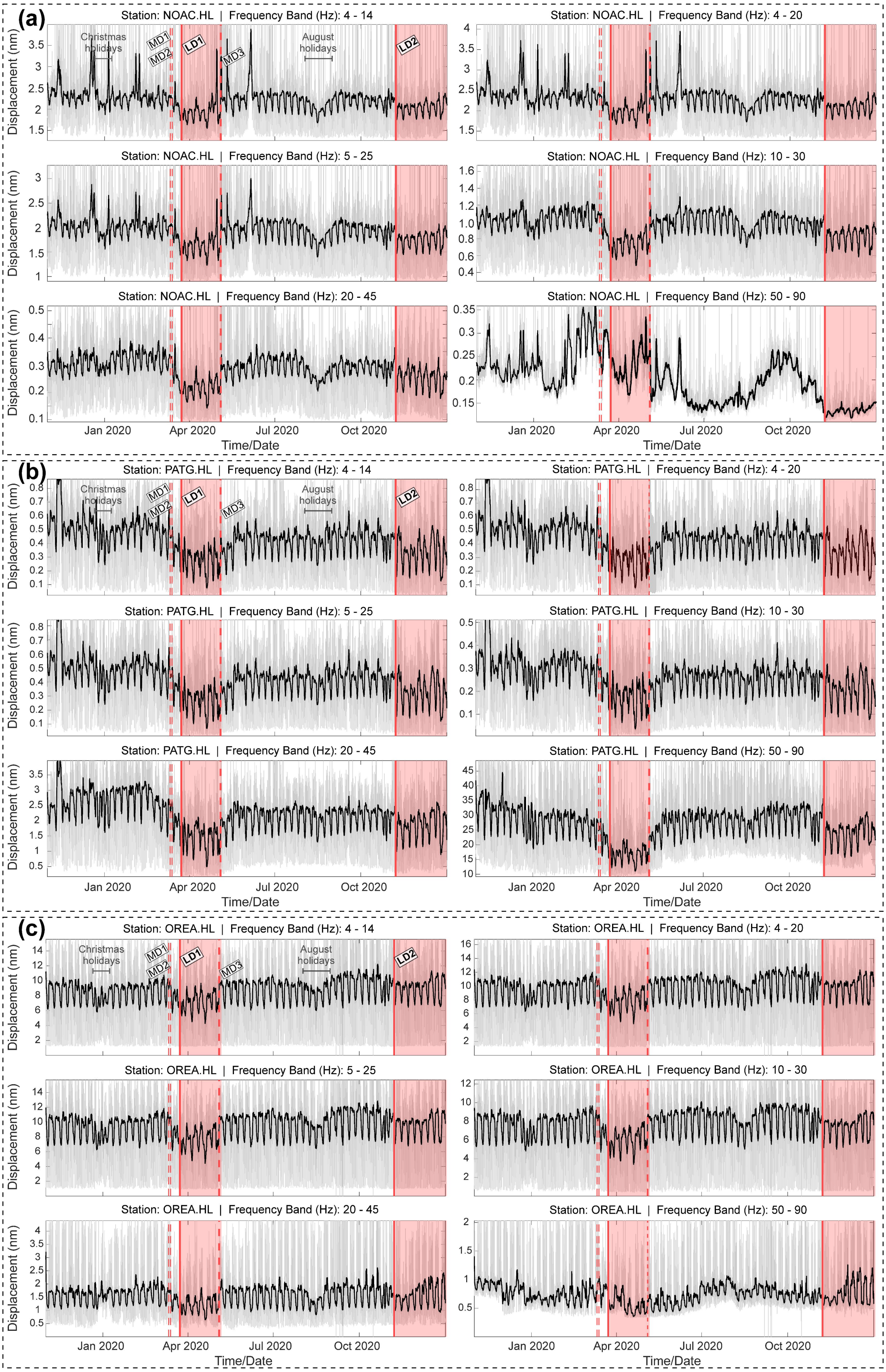

Figure 3 The long-term temporal evolution of HiFSAN is presented in six different frequency bands (4-14 Hz, 4-20 Hz, 5-25 Hz, 10-30 Hz, 20-45 Hz and 50-90 Hz), displayed as ground displacement (vertical component) from stations (a) NOAC, (b) PATG and (c) OREA. The average PPSD computed from thirty-minute windows with a 50 percent overlap is shown in grey, with the moving median (window size: 24 hrs) depicted in black. The initiation of the first (March 23, 2020, LD1) and the second national lockdown (November 4, 2020, LD2) is indicated by solid red lines. Three additional milestone dates (red dashed lines), namely the closure of all educational institutions on March 11, 2020 (MD1), the closure of all shopping centres, cafes, restaurants on March 13, 2020 (MD2) and the initiation of the gradual lifting of the first lockdown measures on May 4, 2020 (MD3), are also marked. The background red color represents the periods when national lockdown measures were in place.

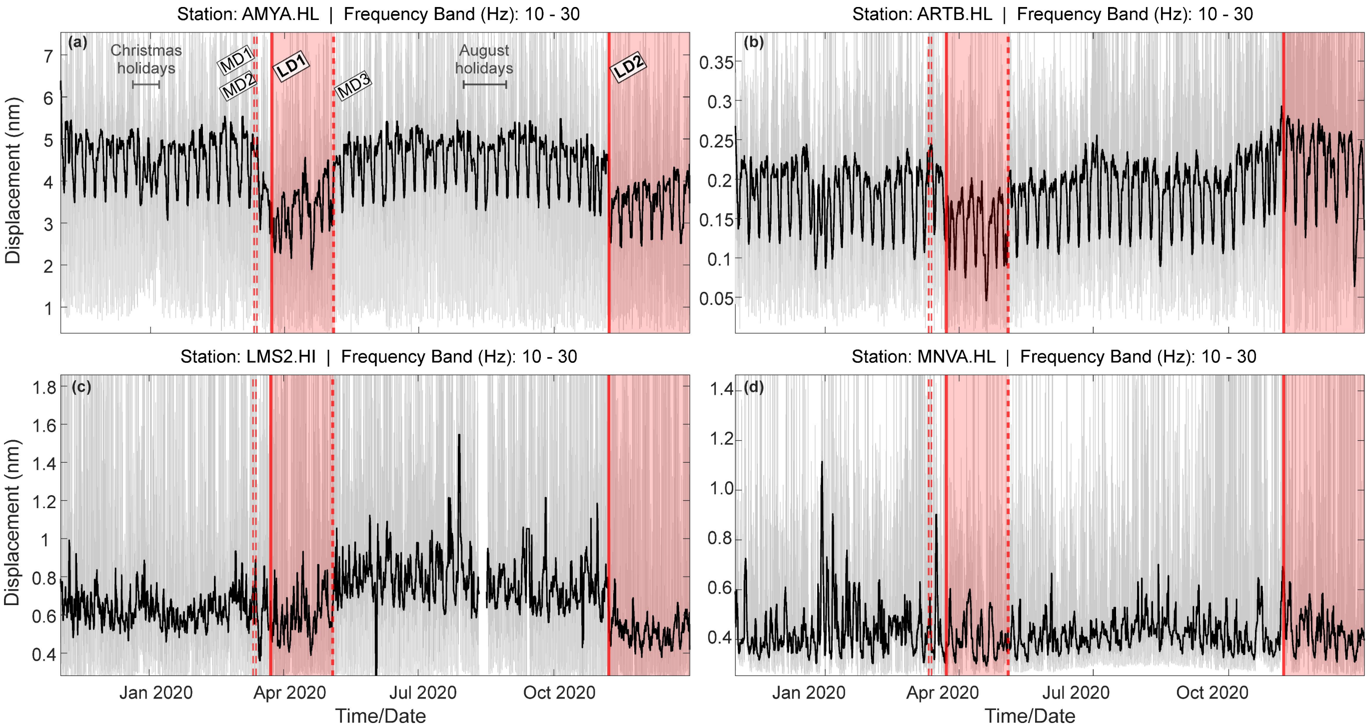

Figure 4 Different trends in the long-term temporal evolution of HiFSAN in the 10-30 Hz frequency band are illustrated for four representative stations. Ground displacement variations (a) at station AMYA, located in the town center of Amyntaio, (b) at station ARTB, located in the city center of Arta, (c) at station LMS2, located in the city center of Lamia and (d) at station MNVA, located in the town center of Monemvasia, are presented. Refer to Figure 3 for the color codes and labels.

within the buildings housing the seismic stations and in the surrounding areas. For example, stations located in buildings that for unknown reasons continued to operate partially during one lockdown but not the other could exhibit such variations. Finally, there are a few stations where zero or negligible noise reductions are observed during both lockdowns, such as the MNVA station (Figure 4d). Compared to stations AMYA and ARTB, stations LMS2 and MNVA do not exhibit clear, typical week-long cycles of seismic noise levels. This could suggest that these stations are less sensitive to periodic anthropogenic sources related to population movements, which may explain why the lockdown effects are less evident or entirely absent in such cases. It is worth noting that all four stations presented in Figure 4 are installed in town/city hall buildings located in the center of their respective towns/cities.

3.2.2 The national median HiFSAN

To gain a comprehensive understanding of HiFSAN variations across the country, the median ground displacement profiles for each station were normalized in the range of 0 to 1 (Figure 5a). The normalization was performed by dividing the displacement time series at each station by the respective maximum amplitude observed during the study period. These normalized profiles were then utilized to derive the national daily median HiFSAN based on ground displacement data (Figure 5b). Despite notable variations in values between different stations, the normalized profiles reveal consistent temporal variation patterns of HiFSAN across the majority of the stations. Focusing on the national daily median HiFSAN (Figure 5b), we observe two significant noise reductions following the initiation of LD1 and LD2 quieting measures. The noise reduction during LD1 appears more pronounced than that observed during LD2. HiFSAN started to progressively decrease approximately ten days before the official onset of the first national lockdown (March 23, 2020, LD1). A gradual reduction in noise followed the implementation of two initial sets of restriction measures: the closure of educational institutions on March 11, 2020 (MD1) and shopping centers and restaurants on March 13, 2020 (MD2). The end of the first strict nationwide lockdown (LD1) on May 4, 2020 (MD3) marked the gradual increase of HiFSAN toward pre-lockdown noise levels.

The lowest noise level during LD1 is reached on Orthodox Easter, particularly on Sunday, 12 April, 2020, while the second-lowest level is observed during the weekend following Christmas Day in 2020 (Friday, 25 December 2020, Figure 5b). These two instances of minimal noise levels in 2020 align with religious holidays that fell within the period when anti-coronavirus containment measures were already in place.

In addition to the lockdown periods, distinct decreases in the national median HiFSAN are evident during the 2019 Christmas and the 2020 New Year holidays, lasting about two weeks (Figure 5b). Furthermore, the August 2020 holidays also stand out as a period of reduced seismic noise levels. Traditionally, the weeks before and after the 15th of August, a national religious holiday in Greece, mark a traditional summer break period. Therefore, the lowest noise level during this holiday period was observed on August 15, 2020 (Figure 5b).

Another noticeable temporal pattern in the median

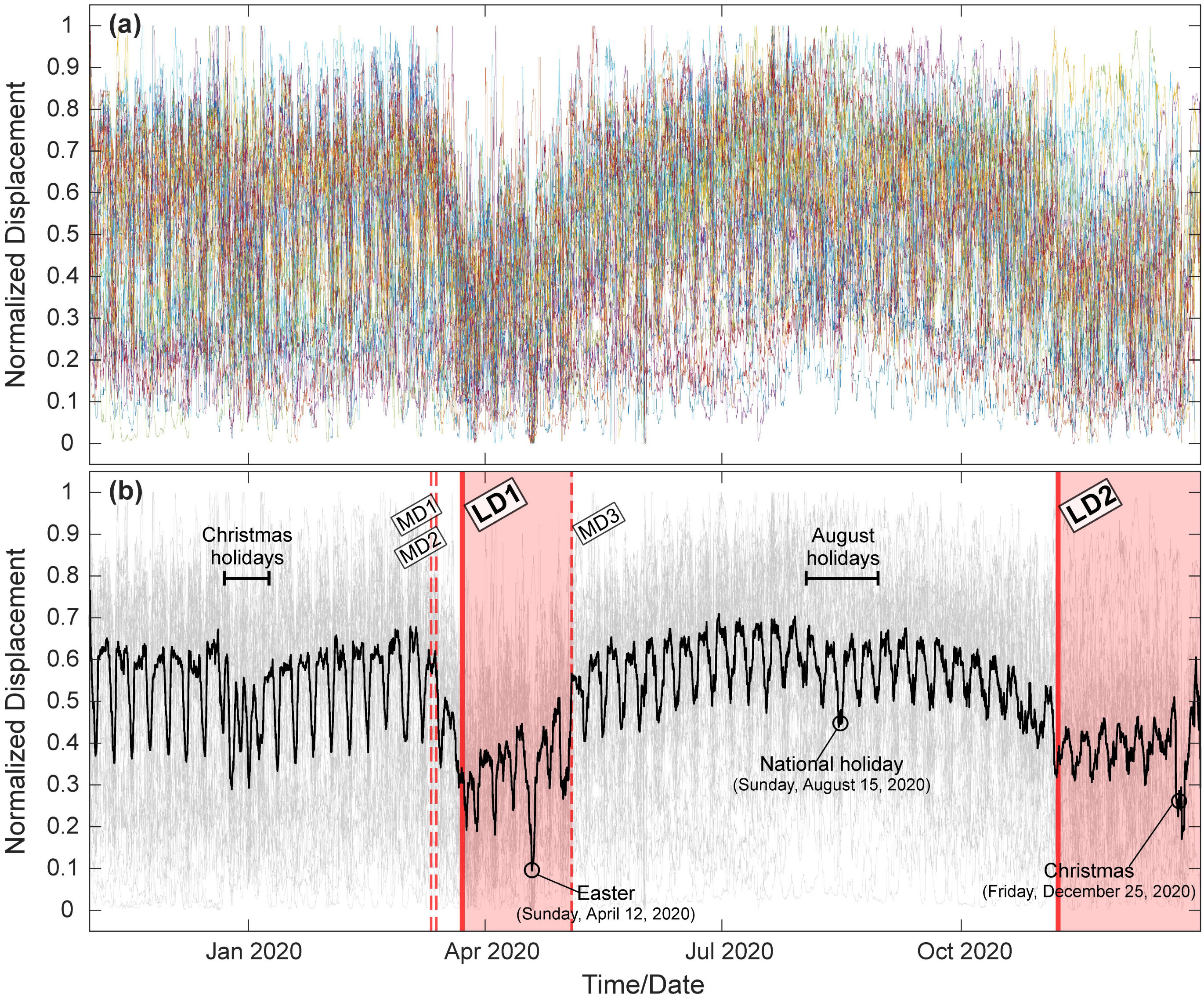

Figure 5 Normalized ground displacement variation in the 10-30 Hz frequency band is depicted for all the investigated stations. (a) The coloured lines represent the daily median of each analysed station. (b) The corresponding normalized median profile (black line) resulted from all the individual station medians (faint grey lines in the background). Refer to Figure 3 for the remaining color codes and labels.

HiFSAN data is the fluctuations between weekdays and weekends, showcasing the typical week-long cycles of seismic noise levels. Consequently, higher HiFSAN values are noted during weekdays, whereas weekends, particularly Sundays, are characterized by local energy minima. This weekday-weekend pattern is evident during both the quarantine period and periods of normal activity (Figure 5b). It is noteworthy that the difference in noise level ranges between weekday and weekend cycles appears to be smaller during the lockdown periods.

3.2.3 HiFSAN percentage changes per station and administrative region

To quantitatively estimate the reductions in HiFSAN across the country, we calculated the percentage change in HiFSAN amplitudes observed at each individual seismic station during the two national lockdowns. This involved computing the median of the HiFSAN during the lockdown periods and the median of the HiFSAN over a period from February 10 to March 10, 2020, chosen to predominantly encompass normal workweeks and exclude any public holidays. The percentage changes are expressed relative to the aforementioned pre-lockdown baseline period.

The percentage variations in HiFSAN observed during the two lockdowns are displayed in map view in Figure 6. Out of a total of 72 strong-motion seismic stations, reductions in HiFSAN during LD1 and LD2 were observed at 65 and 57 stations, respectively. In LD1, 26 stations exhibited a HiFSAN reduction between 0% and 20%, 31 stations showed a reduction ranging between 20% and 40%, and 8 stations demonstrated a reduction exceeding 40%. In LD2, 43 stations had a HiFSAN reduction between 0% and 20%, 20 stations had a HiFSAN reduction between 20% and 40%, and 3 stations had a HiFSAN reduction exceeding 40%. The effect of LD1 was not observed at one station, while the effect of LD2 was not visible at five stations. Stations characterized by large data gaps, operating problems and other data-related is-

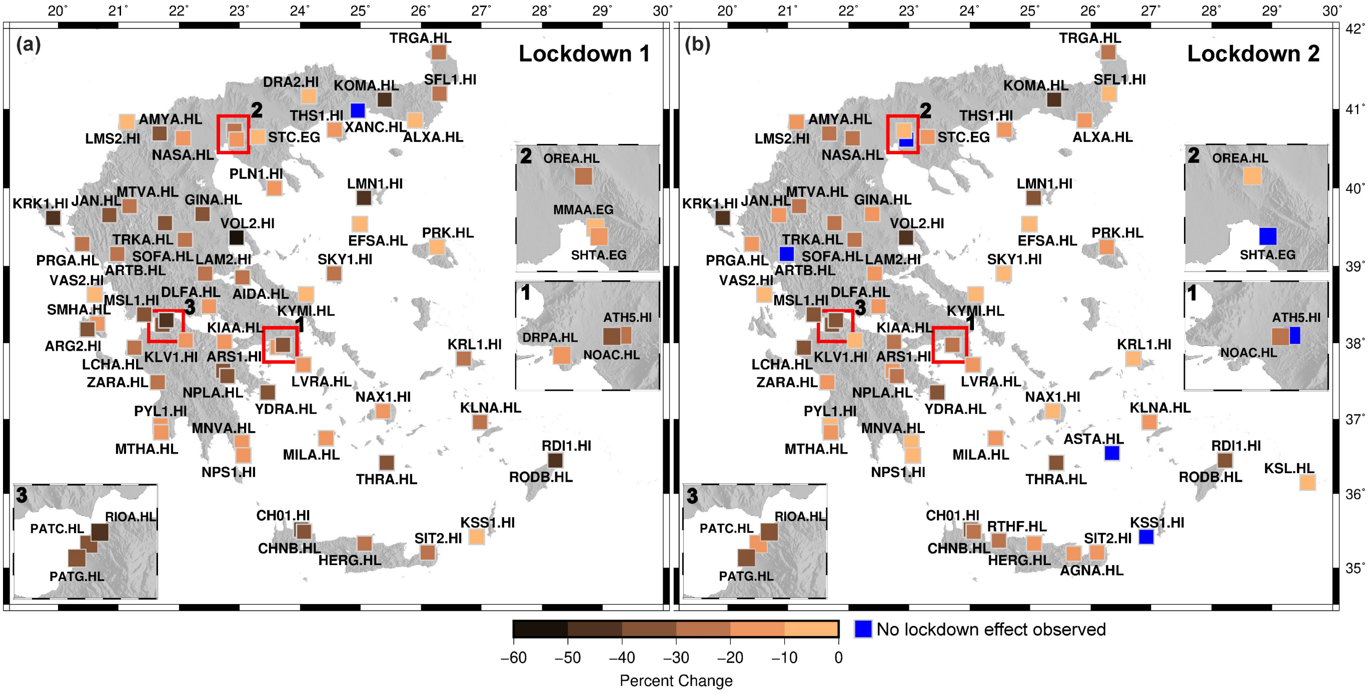

Figure 6 Locations of the analysed strong-motion stations throughout Greece and percent changes in HiFSAN between 10 and 30 Hz, during (a) the first and (b) the second lockdown. Percent changes are expressed relative to a baseline before the first lockdown (February, 10 – March, 10, 2020). Stations experiencing significant data gaps or operating issues over the period of interest are not plotted. Stations where the lockdown effect was not observed are presented by blue squares.

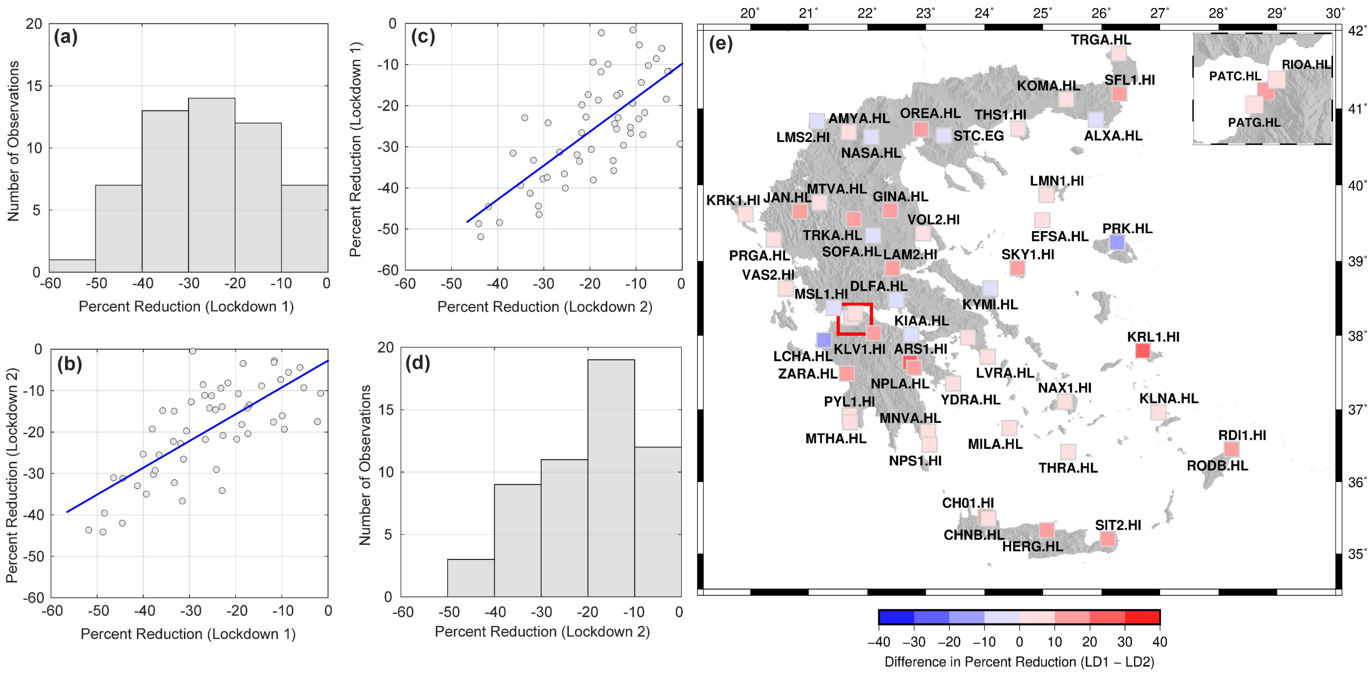

Figure 7 Correlation analysis of percent reductions in seismic noise during the two lockdowns and their differences, as visualized in map view. (a, d) Histograms showing the distribution of percent reductions for each lockdown. (b, c) Scatter plots with regression lines illustrating the linear relationship between the percent reductions observed in the two lockdowns. The correlation coefficient (R) is 0.73, indicating a strong positive relationship. (e) Map view showing the differences in percent reductions between the first and second lockdown at each station. Warm colors (positive values) indicate greater reductions during the first lockdown, while cool colors (negative values) indicate larger reductions during the second lockdown. The differences were calculated only for stations where reductions were observed during both lockdowns.

sues during the periods of interest (i.e., before and after the lockdowns) were excluded from the analysis. Table 2 gives an overview of the seismic stations' response to both lockdowns.

During LD1, the stations that demonstrated reductions in HiFSAN levels exceeding 40% included VOL2 (52%), RIOA (48%), KOMA (48%), RODB (46%), KRK1 (45%), CH01 (44%), LMN1 (41%), and RDI1 (40%). As previously mentioned, during LD2, the number of stations showing such significant reductions decreased to three: VOL2 (44%), KOMA (44%), and KRK1 (42%).

Considering that all stations operate within environments with similar anthropogenic noise characteristics (within urban areas), the variations in HiFSAN levels depicted in Figure 6 do not exhibit any distinct spatial distribution or pattern. It seems that the effects of the lockdowns are not influenced by the stations' locations, whether a station is located in a mainland city/town or on an island.

A possible explanation for the varying responses of different cities during the lockdowns could be differences in population size. Although there is no strong statistical relationship between noise reduction and population size (see supplementary material), a general trend suggests that cities with larger populations are typically associated with higher baseline levels of human activity, which tend to be more significantly suppressed during lockdowns. As a result, areas with larger populations are more likely to exhibit pronounced reductions in seismic noise as human mobility and activity decrease during the lockdowns. The lack of a strong statistical relationship between noise reduction and population size, however, may be attributed to the fact that while population size is a broad-scale factor, high-frequency seismic noise (10–30 Hz) is predominantly influenced by local sources, such as nearby traffic, within a few hundred meters of each station.

Figure 7 examines the relationship between noise reductions during LD1 and LD2, showing a correlation plot (Figure 7a-d) and a map of the spatial distribution of percent reduction differences between the two lockdowns (Figure 7e). The percent reductions of LD1 compared to those of LD2 show a positive linear relationship, with a correlation coefficient of 0.73. This suggests a consistent trend across stations, although noise reductions during the second lockdown are generally smaller than those observed during the first. Exceptions to this general trend are clearly visible in the map of Figure 7e, where positive values (warm colors) indicate larger reductions during the first lockdown, and negative values (cool colors) indicate larger reductions during the second lockdown. While no distinct spatial patterns emerge, a general trend is evident. In larger cities with populations exceeding 100,000, reductions during the first lockdown tend to be more pronounced compared to those of the second. For instance, this is observed at stations such as NOAC (Athens), OREA (Thessaloniki), PATC, PATG, RIOA (Patras), and HERG (Heraklion). In smaller cities, most stations follow the same trend, but some, such as LCHA (Lechaina) and SOFA (Sofades), exhibit greater reductions during the second lockdown. As previously noted, while the correlation between noise reduction and population size lacks strong statistical support, we cautiously observe that business cities with larger populations tend to experience greater reductions in seismic noise levels, particularly during the first lockdown.

Greece is divided into 13 decentralized administrative regions. Using Figure 6, which depicts the percent reductions in seismic noise per station, we grouped the stations spatially by their respective administrative regions to calculate and display the median percent reduction for each region. Figure 8 illustrates the median percent reduction in HiFSAN across the 13 administrative regions of Greece during both lockdowns. At the regional level, trends similar to those observed at the individual station level can be noted. Overall, the most significant reductions in seismic noise were recorded during the first lockdown in the majority of the regions (9 out of 13). Specifically, greater percent reductions during the first lockdown were observed in Central Greece, Peloponnese, Ionian Islands, Thessaly, Epirus, East Macedonia and Thrace, North Aegean, South Aegean, and Crete. In contrast, Attica, Western Greece, Western Macedonia and Central Macedonia exhibited median noise reductions that were approximately 3% higher during the second lockdown compared to the first. Comparing these seismic noise reduction data with mobility data could provide valuable insights into interpreting these variations. However, Google's mobility data are available for only 7 decentralized regions, which differ significantly from Greece's 13 administrative regions, complicating a direct comparison between seismic noise and mobility patterns. Furthermore, the mobility data for 5 of these 7 regions contain gaps across several categories, limiting their utility. Consequently, such a comparison is feasible only at the national level and is presented in Section 3.3.

3.2.4 Collocated seismometer – accelerometer comparison

To further emphasize the effectiveness of accelerometers in monitoring changes in anthropogenic activity, we conducted a comparison between the results obtained from a broadband sensor and the co-located strong-motion sensor. Specifically, we analyzed and compared the temporal changes in HiFSAN at the NOAC.HL strong-motion sensor and the ATH.HL broadband station. Station ATH is installed in the city center of Athens within the facilities of the Institute of Geodynamics of the National Observatory of Athens and is equipped with a Streckeisen STS-2 broadband sensor, acquiring data at a sampling rate of 100 sps. The analysis reveals remarkably similar HiFSAN variations between both co-located stations (Figure 9). Both lockdowns and other periods characterized by lower seismic noise (such as the Christmas and August holidays) are clearly identified in both datasets. To quantify the similarity between the two time series, a correlation analysis was also performed using the common Pearson correlation coefficient. The correlation coefficients between the ground displacement data as well as their corresponding moving median (window size 24 hrs) exhibit a value of 0.938 and 0.985, respectively. A detailed comparative analysis between seismometer and accelerometer data could certainly constitute an independent area of study. However, the aforementioned comparison supports the assumption that strong-motion sensors can effectively monitor variations in anthropogenic noise, thereby reflecting variations in human activity.

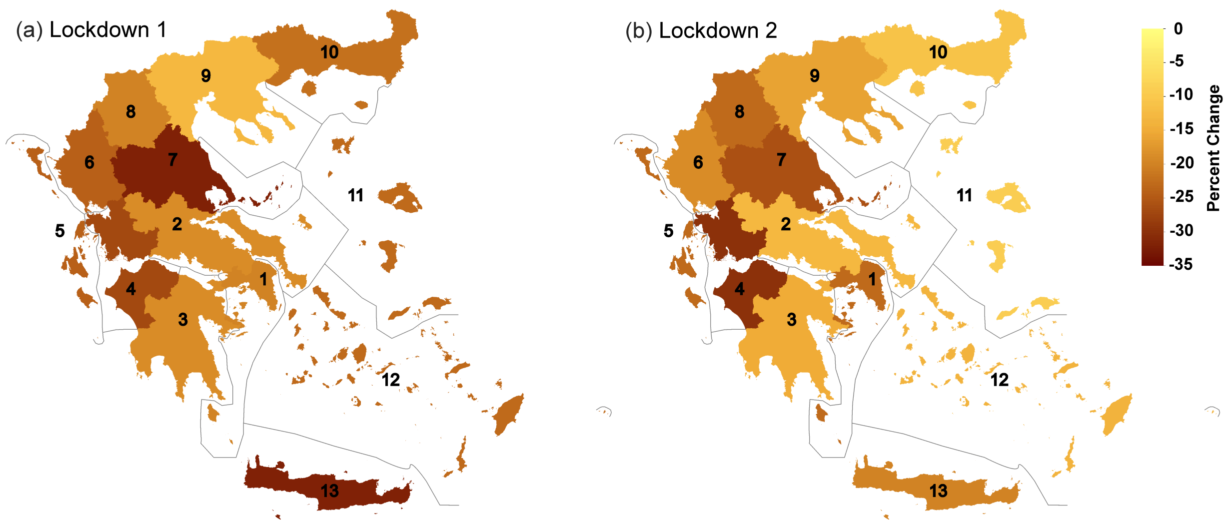

Figure 8 Median percent changes in HiFSAN during (a) the first lockdown and (b) the second lockdown, across the 13 administrative regions of Greece. Median values were calculated based on the noise reductions per station presented in Figure 6. The numbers on the maps correspond to the respective administrative regions of Greece: 1. Attica, 2. Central Greece, 3. Peloponnese, 4. Western Greece, 5. Ionian Islands, 6. Epirus, 7. Thessaly, 8. Western Macedonia, 9. Central Macedonia, 10 East Macedonia and Thrace, 11 North Aegean, 12 South Aegean, and 13. Crete.

	LD1	LD2
No. of stations from which the initial dataset was acquired.	72	72
No. of stations excluded from the analysis (large data gaps, operating issues etc.).	6	10
No. of stations where lockdown effect was not observed.	1	5
No. of stations where lockdown effect was observed.	65	57

Table 2 An overview of the strong-motion stations' response to both lockdowns (LD1, LD2).

3.3 Comparison with human mobility data and the national response to COVID-19 lockdowns

The previous analysis demonstrates that the temporal evolution of HiFSAN in the 10-30 Hz frequency band can serve as an effective indicator to track changes in human activity within urban environments. To further evaluate the practical utility of seismic data as a monitoring tool, we compare our results with data describing the mobility of citizens. Following the beginning of the COVID-19 pandemic, major technology companies, such as Google, Apple, and Meta, have released mobility data reports. In this study, we focus on the mobility data provided by Google through the Community COVID-19 Mobility Reports (Google, 2022). These reports provide insights into mobility patterns since February 15, 2020. The data are derived from anonymized and aggregated location information sourced from mobile phones, providing daily percentage changes across various mobility categories. These categories include mobility related to public transportation, movement for residential visits, retail and recreation activities and commuting to and from workplaces. Changes reported by Google are expressed as daily percentage changes relative to a baseline established before the lockdown period (Google, 2022).

A visual comparison between changes in HiFSAN and the corresponding mobility data is presented in Figure 10. The percentage change in HiFSAN is also expressed relative to a baseline before the first lockdown. Each data point on the HiFSAN graph (Figure 10) represents the daily percentage change from the median HiFSAN observed during a period of normal activity before the first lockdown between February 10 and March 10, 2020. As mentioned in the previous section, this period of normal activity is characterized by typical working days, regular weekends, and the absence of public holidays. As anticipated, there is a notable similarity among the various human mobility patterns, all underscoring a decrease in human activity during both lockdown periods. Moreover, with the exception of one instance, the resemblance between HiFSAN and human mobility patterns appears to be remarkably high (Figure 10). All categories of citizen mobility exhibit a strong positive correlation, with the exception of time spent on residential visits, which shows an anti-correlation.

Specifically, mobility data associated with workplaces (yellow line in Figure 10), transportation (orange line in Figure 10) and retail and recreation (blue line in Figure 10) display similar patterns, marked by an initial decrease after MD1 and MD2 (pre-LD1 restriction measures), reaching their lowest values following the onset of LD1. Before the full implementation of LD1, the initial containment measures that were put in place included the closure of all educational institutions on March 11, 2020 (MD1) and the closure of all shopping centers, cafes and restaurants on March 13, 2020 (MD2).

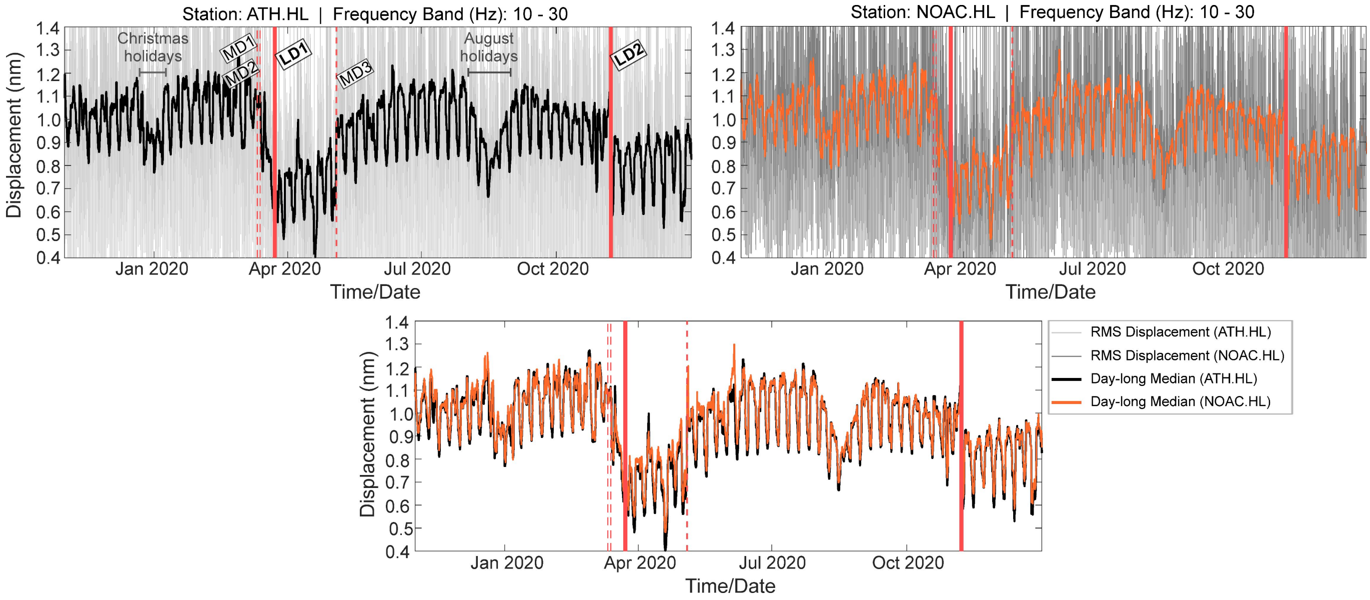

Figure 9 Comparison of the long-term temporal evolution of HiFSAN in the 10-30 Hz frequency band derived from (a) velocity data (station ATH) and (b) acceleration data (station NOAC). HiFSAN is presented as ground displacement. Average PPSD was computed from thirty-minute windows with a 50 percent overlap (light grey and dark grey for station ATH and station NOAC, respectively). The moving median (window size 24 hrs) is shown in thick black and thick orange, for station ATH and station NOAC, respectively. Refer to Figure 3 for the remaining color codes and labels.

Following these measures, a gradual reduction of HiFSAN, mirroring the corresponding gradual reduction in mobility, was observed.

On March 23, 2020, the first nationwide lockdown was imposed, significantly restricting citizens' mobility. From that point until the official end of LD1, HiFSAN levels consistently remained low. HiFSAN levels appear to have decreased by 43% nationally during the entire LD1 period. The first lockdown period is also characterized by the presence of a substantial reduction in seismic noise levels of just over 80%, which was recorded on 2020 Easter Sunday (April 21, 2020). The simultaneous occurrence of two periods of limited mobility, LD1 restriction measures and the 2020 Easter holiday, contributed to this remarkable reduction in HiFSAN.

Following the end of LD1, HiFSAN began to progressively return to pre-lockdown levels, achieving a full rebound approximately one month after the official end of LD1. This pattern aligns with observations in the mobility data as well (Figure 10).

During the 2020 summer season, there were typically no restrictions on the movement of citizens. However, as mentioned in the previous sections, a distinct decrease in HiFSAN is observed, especially during August. This observation aligns with the significant reduction in citizens' mobility in relation to workplaces during August, as is evident from mobility data (Figure 10). Mobility linked to workplaces shows a gradual decline starting from July and continuing until mid-August, when it reaches a local minimum. In particular, the most significant decrease in seismic noise levels during the 2020 summer season, amounting to 25%, was observed on August 15, 2020. This observation is not coincidental, as August 15 is an official holiday in Greece, with many employees taking time off for their summer holidays. From mid-August onwards, mobility progressively tends to reach pre-summer values. While the overall trend between mobility data and seismic noise is generally consistent, a closer look at periods outside the lockdowns, particularly during the tourist season, reveals unexpectedly high workplace mobility during weekends. A possible explanation is that Google's workplace mobility data may unknowingly capture other types of movement across the country that do not strictly correspond to workplace-related activities.

In October 2020, approximately one month before the onset of LD2, a gradual decrease in HiFSAN levels is noticeable. Despite the absence of official government restrictions on citizens' mobility during this period, the decrease in seismic noise levels correlates with the emergence of a severe second wave of COVID-19 cases. This could suggest that citizens may have informally adopted self-protection measures, such as limiting their movements, in response to the worsening pandemic situation. The adoption of self-protection measures is also evident in the mobility data, which show a similar decreasing trend to that observed in the noise data (Figure 10).

Following the official implementation of LD2, HiFSAN levels experienced a significant reduction of 36%. This trend is also reflected in citizens' mobility data. Overall, the percentage reduction observed during LD2 in both seismic noise levels and mobility data is less pronounced compared to the first lockdown. On Christmas Day 2020, which coincided with the second lockdown, a substantial reduction of approximately 70% was observed, marking the second largest reduction recorded during 2020. While the reductions in HiFSAN, especially during the two lockdown periods, follow a similar trend and correlate positively with changes in different categories of citizens' mobility, the actual percentage reductions between them differ. Examining Figure

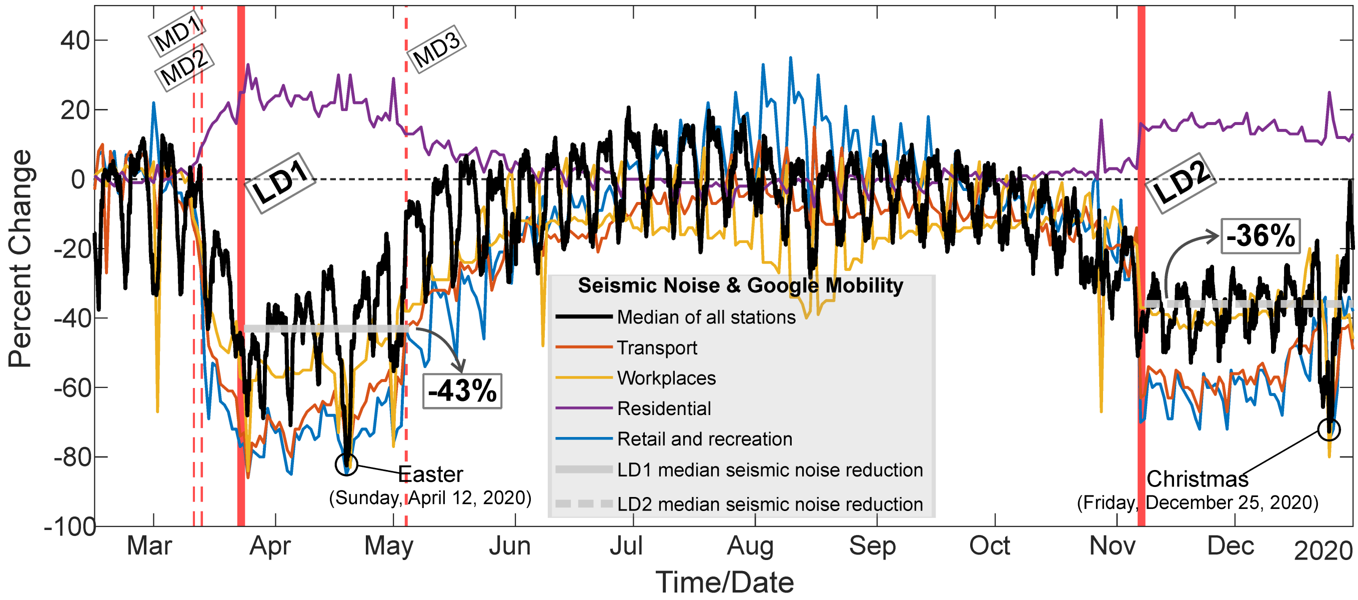

Figure 10 Comparison between temporal percent changes in national-scale daily median HiFSAN and citizen mobility data provided by Google. The national-scale daily median HiFSAN is based on data from stations where the lockdown effects were observed. The percent changes of HiFSAN are expressed relative to a baseline before the first lockdown (February, 10 - March, 10, 2020). The initiation of the first (March 23, 2020, LD1) and the second national lockdown (November 4, 2020, LD2) are shown as solid red lines. Three additional milestone dates (red dashed lines), namely the closure of all educational institutions on March 11, 2020 (MD1), the closure of all shopping centres, cafes, restaurants on March 13, 2020 (MD2) and the initiation of the gradual lifting of the first lockdown measures on May 4, 2020 (MD3) are also shown.

10, it becomes evident that the reductions in mobility data related to retail (blue line) and transportation (orange line) during the two lockdowns are approximately 30% greater than that captured by the seismic noise data. This variance could be attributed to the fact that most stations are installed closer to workplaces (e.g., town halls, public services, administrative offices, etc.) rather than traffic and retail sites. This also explains why mobility data related to workplaces (yellow line) better coincide with the noise data. Overall, another explanation of the observed variance on a national scale could be the extensive volume of mobility data sourced from mobile phone users, offering a significantly dense spatial coverage compared to the comparatively limited spatial coverage provided by seismological networks. Mobility data related to residential visits (purple line in Figure 10), unlike the other mobility categories, systematically exhibits increased values when restriction measures were in place during both lockdown periods. This observation is normally expected, due to the increased number of citizens spending more time at places of residence as a result of the government stay-at-home orders.

4 Conclusions

In 2020, the COVID-19 pandemic and the subsequent implementation of two nationwide lockdowns had a profound impact on high-frequency seismic ambient noise levels in Greece. We exclusively utilized continuous seismic data from strong-motion seismic sensors from urban areas throughout Greece to investigate variations in seismic noise levels during the pandemic period. The effects of the lockdown measures were clearly observed at the majority of the seismic stations. Our analysis revealed that the implementation of the lockdowns resulted in significant reductions in HiFSAN levels, with a remarkable reduction of 43% observed during the first lockdown and a substantial reduction of 36% observed during the second lockdown. These reductions were particularly prominent at frequencies above 4 Hz, characteristic of anthropogenic seismic noise, and were evident across all studied frequency bands, including the 10-30 Hz range, which was the primary focus of the current study to facilitate result visualization. Notably, Easter Sunday 2020 and Christmas Day 2020 were recognized as periods characterized by significant reductions in seismic noise levels, with reductions exceeding 80% and 70%, respectively. The 2020 lockdowns led to the most extensive reduction in seismic noise levels ever recorded in Greece. Although the same restriction measures were implemented during both lockdowns, the reduction in seismic noise levels was more pronounced during the first lockdown than the second. This observation aligns with Google mobility data, which show higher levels of human mobility during the second lockdown. A plausible explanation for this difference is that citizens may have been less motivated to strictly follow the restriction measures during the second lockdown, leading to increased mobility. This behavioral shift is reflected in both the mobility and seismic data. The median results of our analysis can adequately reproduce human activity patterns, especially workplaces' mobility, as evident from citizens' mobility data. This confirms that high frequency seismic data can serve as a reliable proxy for monitoring anthropogenic activity at a city scale. Moreover, we highlight the applicability of strong-motion instruments as effective tools for monitoring social activity in urban environments. There have been several studies investigating the seismic impact of various human-related activities within urban environments (Riahi and Gerstoft, 2015; Green et al., 2016; Sheen et al., 2009; Diaz et al., 2020; Díaz et al., 2017), highlighting the different roles that city-based seismic sensors can fulfill (e.g., seismological, educational). However, the global-scale containment of humans' socio-economic activity during the COVID-19 pandemic has significantly emphasized the complementary use of seismic deployments and further development in the relevant field of seismology, known as Social Seismology.

Data and code availability

The waveform data and related metadata utilized in this study are publicly available and were acquired from the HL (National Observatory of Athens, Institute of Geodynamics, Athens, 1975), HI ((ITSAK) Institute of Engineering Seimology Earthquake Engineering, 1981) and EG (Aristotle University of Thessaloniki, 1993) networks that were accessed through the National Observatory of Athens data center node (EIDA@NOA, http://eida.gein.noa.gr) (Evangelidis et al., 2021). The mobility data used in this paper are also publicly available through Google's COVID-19 Community Mobility Report (Google, 2022).

Acknowledgements

The original idea for the seismic noise analysis in relation to the COVID-19 lockdown measures is from Thomas Lecocq. We gratefully acknowledge the Handling Editor Lise Retailleau and two anonymous reviewers for their constructive comments, which have helped us to improve the clarity and completeness of this study. We also thank Panagiota Kokkali (Hellenic Survey of Geology & Mineral Exploration - HSGME) for her assistance in the creation of Figure 8. The calculation of the temporal variation of the seismic ground motion displacement RMS and the overall seismic noise analysis was performed by using the ObsPy implementation (Krischer et al., 2015) and the open-access software package SeismoRMS (Lecocq et al., 2020b). Maps were drawn by using the open-sourced Generic Mapping Tools (GMT) software (Wessel et al., 2013). Diagram plots were created using MATLAB (Matlab and Statistics Toolbox Release 2021a, The MathWorks, Inc., Natick, Massachusetts, United States).

Competing interests

The authors have no competing interests.

References

Aristotle University of Thessaloniki. EUROSEISTEST Strong Motion Network [Data set], 1993. https://www.fdsn.org/networks/detail/EG/.

Arroyo-Solórzano, M., Castro-Rojas, D., Massin, F., Linkimer, L., Arroyo, I., and Yani, R. COVID-19 lockdown effects on the seismic recordings in Central America. *Solid Earth*, 12(10):2127–2144, 2021. doi: 10.5194/se-12-2127-2021.

Boginskaya, N. V. and Kostylev, D. V. Change in the Level of Microseismic Noise During the COVID-19 Pandemic in the Russian Far East. *Pure and Applied Geophysics*, 179(11):4207–4219, Nov 2022. doi: 10.1007/s00024-022-03019-7.

Bonnefoy-Claudet, S., Cotton, F., and Bard, P.-Y. The nature of noise wavefield and its applications for site effects studies: A literature review. *Earth-Science Reviews*, 79(3):205–227, 2006. doi: 10.1016/j.earscirev.2006.07.004.

Cannata, A., Cannavò, F., Di Grazia, G., Aliotta, M., Cassisi, C., De Plaen, R. S. M., Gresta, S., Lecocq, T., Montalto, P., and Sciotto, M. Seismic evidence of the COVID-19 lockdown measures: a case study from eastern Sicily (Italy). *Solid Earth*, 12(2): 299–317, 2021. doi: 10.5194/se-12-299-2021.

Curtis, A., Gerstoft, P., Sato, H., Snieder, R., and Wapenaar, K. Seismic interferometry—turning noise into signal. *The Leading Edge*, 25(9):1082–1092, 2006. doi: 10.1190/1.2349814.

De Plaen, R. S. M., Márquez-Ramírez, V. H., Pérez-Campos, X., Zuñiga, F. R., Rodríguez-Pérez, Q., Gómez González, J. M., and Capra, L. Seismic signature of the COVID-19 lockdown at the city scale: a case study with low-cost seismometers in the city of Querétaro, Mexico. *Solid Earth*, 12(3):713–724, 2021. doi: 10.5194/se-12-713-2021.

Díaz, J., Ruiz, M., Sánchez-Pastor, P. S., and Romero, P. Urban Seismology: on the origin of earth vibrations within a city. *Scientific Reports*, 7(1):15296, Nov 2017. doi: 10.1038/s41598-017-15499-y.

Diaz, J., Schimmel, M., Ruiz, M., and Carbonell, R. Seismometers Within Cities: A Tool to Connect Earth Sciences and Society. *Frontiers in Earth Science*, Volume 8 - 2020, 2020. doi: 10.3389/feart.2020.00009.

Diaz, J., Ruiz, M., and Jara, J.-A. Seismic monitoring of urban activity in Barcelona during the COVID-19 lockdown. *Solid Earth*, 12(3):725–739, 2021. doi: 10.5194/se-12-725-2021.

Evangelidis, C. P. and Melis, N. S. Ambient Noise Levels in Greece as Recorded at the Hellenic Unified Seismic Network. *Bulletin of the Seismological Society of America*, 102(6):2507–2517, 12 2012. doi: 10.1785/0120110319.

Evangelidis, C. P., Triantafyllis, N., Samios, M., Boukouras, K., Kontakos, K., Ktenidou, O., Fountoulakis, I., Kalogeras, I., Melis, N. S., Galanis, O., Papazachos, C. B., Hatzidimitriou, P., Scordilis, E., Sokos, E., Paraskevopoulos, P., Serpetsidaki, A., Kaviris, G., Kapetanidis, V., Papadimitriou, P., Voulgaris, N., Kassaras, I., Chatzopoulos, G., Makris, I., Vallianatos, F., Kostantinidou, K., Papaioannou, C., Theodoulidis, N., Margaris, B., Pilidou, S., Dimitriadis, I., Iosif, P., Manakou, M., Roumelioti, Z., Pitilakis, K., Riga, E., Drakatos, G., Kiratzi, A., and Tselentis, G. Seismic Waveform Data from Greece and Cyprus: Integration, Archival, and Open Access. *Seismological Research Letters*, 92(3):1672–1684, 03 2021. doi: 10.1785/0220200408.

Giannopoulos, D., Evangelidis, C., Lois, A., Sokos, E., and Lecocq, T. The footprint of "lockdown" measures to curb COVID-19 spread in Greece on seismic noise, Sept. 2021. https://doi.org/10.5281/zenodo.7424040.

Giannopoulos, D., Vallianatos, F., Lois, A., and Hloupis, G. Non-extensive statistical physics analysis of high-frequency anthropogenic seismic noise with relation to COVID-19 pandemic lockdown measures: Preliminary observations, Dec. 2022. https://doi.org/10.5281/zenodo.7424070.

Google. COVID-19 Community Mobility Reports. https://www.google.com/covid19/mobility/, 2022. [Last Accessed 17

October 2022].

Grecu, B., Borleanu, F., Tiganescu, A., Poiata, N., Dinescu, R., and Tataru, D. The effect of 2020 COVID-19 lockdown measures on seismic noise recorded in Romania. *Solid Earth*, 12(10): 2351–2368, 2021. doi: 10.5194/se-12-2351-2021.

Green, D. N., Bastow, I. D., Dashwood, B., and Nippress, S. E. J. Characterizing Broadband Seismic Noise in Central London. *Seismological Research Letters*, 88(1):113–124, 10 2016. doi: 10.1785/0220160128.

Gualtieri, L., Stutzmann, E., Capdeville, Y., Ardhuin, F., Schimmel, M., Mangeney, A., and Morelli, A. Modelling secondary microseismic noise by normal mode summation. *Geophysical Journal International*, 193(3):1732–1745, 04 2013. doi: 10.1093/gji/ggt090.

(ITSAK) Institute of Engineering Seimology Earthquake Engineering. ITSAK Strong Motion Network [Data set], 1981. https://www.fdsn.org/networks/detail/HI/.

Krischer, L., Megies, T., Barsch, R., Beyreuther, M., Lecocq, T., Caudron, C., and Wassermann, J. ObsPy: a bridge for seismology into the scientific Python ecosystem. *Computational Science & Discovery*, 8(1):014003, may 2015. doi: 10.1088/1749-4699/8/1/014003.

Lecocq, T., Hicks, S. P., Noten, K. V., van Wijk, K., Koelemeijer, P., Plaen, R. S. M. D., Massin, F., Hillers, G., Anthony, R. E., Apoloner, M.-T., Arroyo-Solórzano, M., Assink, J. D., Büyükakpınar, P., Cannata, A., Cannavo, F., Carrasco, S., Caudron, C., Chaves, E. J., Cornwell, D. G., Craig, D., den Ouden, O. F. C., Diaz, J., Donner, S., Evangelidis, C. P., Evers, L., Fauville, B., Fernandez, G. A., Giannopoulos, D., Gibbons, S. J., Girona, T., Grecu, B., Grunberg, M., Hetényi, G., Horleston, A., Inza, A., Irving, J. C. E., Jamalreyhani, M., Kafka, A., Koymans, M. R., Labedz, C. R., Larose, E., Lindsey, N. J., McKinnon, M., Megies, T., Miller, M. S., Minarik, W., Moresi, L., Márquez-Ramírez, V. H., Möllhoff, M., Nesbitt, I. M., Niyogi, S., Ojeda, J., Oth, A., Proud, S., Pulli, J., Retailleau, L., Rintamäki, A. E., Satriano, C., Savage, M. K., Shani-Kadmiel, S., Sleeman, R., Sokos, E., Stammler, K., Stott, A. E., Subedi, S., Sørensen, M. B., Taira, T., Tapia, M., Turhan, F., van der Pluijm, B., Vanstone, M., Vergne, J., Vuorinen, T. A. T., Warren, T., Wassermann, J., and Xiao, H. Global quieting of high-frequency seismic noise due to COVID-19 pandemic lockdown measures. *Science*, 369(6509):1338–1343, 2020a. doi: 10.1126/science.abd2438.

Lecocq, T., Massin, F., Satriano, C., Vanstone, M., and Megies, T. SeismoRMS - A simple python/jupyter notebook package for studying seismic noise changes. https://doi.org/10.5281/zenodo.3820046. doi: 10.5281/zenodo.3820046.

Li, Q., Guan, X., Wu, P., Wang, X., Zhou, L., Tong, Y., Ren, R., Leung, K. S., Lau, E. H., Wong, J. Y., Xing, X., Xiang, N., Wu, Y., Li, C., Chen, Q., Li, D., Liu, T., Zhao, J., Liu, M., Tu, W., Chen, C., Jin, L., Yang, R., Wang, Q., Zhou, S., Wang, R., Liu, H., Luo, Y., Liu, Y., Shao, G., Li, H., Tao, Z., Yang, Y., Deng, Z., Liu, B., Ma, Z., Zhang, Y., Shi, G., Lam, T. T., Wu, J. T., Gao, G. F., Cowling, B. J., Yang, B., Leung, G. M., and Feng, Z. Early Transmission Dynamics in Wuhan, China, of Novel Coronavirus–Infected Pneumonia. *New England Journal of Medicine*, 382(13):1199–1207, 2020. doi: 10.1056/NEJMoa2001316.

McNamara, D. E. and Buland, R. P. Ambient Noise Levels in the Continental United States. *Bulletin of the Seismological Society of America*, 94(4):1517–1527, 08 2004. doi: 10.1785/012003001.

McNamara, D. E., Hutt, C. R., Gee, L. S., Benz, H. M., and Buland, R. P. A Method to Establish Seismic Noise Baselines for Automated Station Assessment. *Seismological Research Letters*, 80 (4):628–637, 07 2009. doi: 10.1785/gssrl.80.4.628.

Ministry of Health. The totality of the legislation applied is available at:. https://covid19.gov.gr/nomothesia-gia-ton-covid-19/, 2022. [Last Accessed October 15, 2022].

National Observatory of Athens, Institute of Geodynamics, Athens. National Observatory of Athens Seismic Network, 1975. https://www.fdsn.org/networks/detail/HL/.

Ojeda, J. and Ruiz, S. Seismic noise variability as an indicator of urban mobility during the COVID-19 pandemic in the Santiago metropolitan region, Chile. *Solid Earth*, 12(5):1075–1085, 2021. doi: 10.5194/se-12-1075-2021.

Paul, A., Campillo, M., Margerin, L., Larose, E., and Derode, A. Empirical synthesis of time-asymmetrical Green functions from the correlation of coda waves. *Journal of Geophysical Research: Solid Earth*, 110(B8), 2005. doi: 10.1029/2004JB003521.

Pérez-Campos, X., Espíndola, V. H., González-Ávila, D., Zanolli Fabila, B., Márquez-Ramírez, V. H., De Plaen, R. S. M., Montalvo-Arrieta, J. C., and Quintanar, L. The effect of confinement due to COVID-19 on seismic noise in Mexico. *Solid Earth*, 12(6): 1411–1419, 2021. doi: 10.5194/se-12-1411-2021.

Poli, P., Boaga, J., Molinari, I., Cascone, V., and Boschi, L. The 2020 coronavirus lockdown and seismic monitoring of anthropic activities in Northern Italy. *Scientific Reports*, 10(1):9404, Jun 2020. doi: 10.1038/s41598-020-66368-0.

Riahi, N. and Gerstoft, P. The seismic traffic footprint: Tracking trains, aircraft, and cars seismically. *Geophysical Research Letters*, 42(8):2674–2681, 2015. doi: 10.1002/2015GL063558.

Sheen, D.-H., Shin, J. S., Kang, T.-S., and Baag, C.-E. Low frequency cultural noise. *Geophysical Research Letters*, 36(17), 2009. doi: 10.1029/2009GL039625.

Somala, S. N. Seismic noise changes during COVID-19 pandemic: a case study of Shillong, India. *Natural Hazards*, 103(1): 1623–1628, Aug 2020. doi: 10.1007/s11069-020-04045-1.

Stutzmann, E., Roult, G., and Astiz, L. GEOSCOPE Station Noise Levels. *Bulletin of the Seismological Society of America*, 90(3): 690–701, 06 2000. doi: 10.1785/0119990025.

Welch, P. The use of fast Fourier transform for the estimation of power spectra: A method based on time averaging over short, modified periodograms. *IEEE Transactions on Audio and Electroacoustics*, 15(2):70–73, 1967. doi: 10.1109/TAU.1967.1161901.

Wessel, P., Smith, W. H. F., Scharroo, R., Luis, J., and Wobbe, F. Generic Mapping Tools: Improved Version Released. *Eos, Transactions American Geophysical Union*, 94(45):409–410, 2013. doi: 10.1002/2013EO450001.

Xiao, H., Eilon, Z. C., Ji, C., and Tanimoto, T. COVID-19 Societal Response Captured by Seismic Noise in China and Italy. *Seismological Research Letters*, 91(5):2757–2768, 08 2020. doi: 10.1785/0220200147.

Yabe, S., Imanishi, K., and Nishida, K. Two-step seismic noise reduction caused by COVID-19 induced reduction in social activity in metropolitan Tokyo, Japan. *Earth, Planets and Space*, 72(1): 167, Nov 2020. doi: 10.1186/s40623-020-01298-9.

The article *The impact of COVID-19 lockdown measures on high-frequency seismic ambient noise in Greece: Utilizing strong-motion seismograph networks for human activity monitoring in urban environments* © 2025 by Dimitrios Giannopoulos is licensed under CC BY 4.0.